PHILOSOPHICAL TRANSACTIONS OF THE ROYAL SOCIETY A MATHEMATICAL, PHYSICAL & ENGINEERING SCIENCES

The Symmetry and Interfacial Structure of Bicrystals

R. C. Pond and W. Bollmann

Phil. Trans. R. Soc. Lond. A 1979 **292**, 449-472
doi: 10.1098/rsta.1979.0069

THE SYMMETRY AND INTERFACIAL STRUCTURE OF BICRYSTALS

By R. C. POND† and W. BOLLMANN‡

† *Department of Metallurgy and Materials Science, University of Liverpool, P.O. Box* 147, *Liverpool L*69 3*BX, U.K.*

‡ *Battelle Institute, Geneva, Switzerland.*

(*Communicated by Sir Charles Frank, F.R.S. – Received* 18 *October* 1978)

CONTENTS

It is shown that the point and space symmetry of bicrystals can be classified according to established schemes of symmetry groups. The symmetry of the pattern created by the lattices of two crystals comprising a bicrystal is considered first. This symmetry depends on the symmetry of the component lattices and their relative orientation and position. A space group can be assigned to such a pattern by using the schemes of crystallographic rods, crystallographic layers, or conventional space groups (Shubnikov & Koptsik 1974) respectively, according to whether one, two or three non-collinear translation symmetry axes are present in the pattern. Patterns are considered to be dichromatic by regarding one lattice arbitrarily as white and the other black; space

Vol. 292. A 1395. 45 [Published 23 October 1979

groups can then be expressed by using colour symmetry formulation. The variation of the symmetry of dichromatic patterns as the component lattices are displaced relatively is discussed. For a pattern with fixed relative orientation of the component lattices the number of non-collinear translation axes is invariant to changes of relative position. However, the point symmetry of the pattern varies according to a conservation rule; the product $n_j r_j$ is invariant with relative displacement where n_j is the numerical expression of the point symmetry for the pattern created by a given relative displacement away from a holosymmetric pattern and r_j is the number of crystallographically equivalent patterns obtained by symmetry related displacements. The product is equal to n_h, the numerical expression of the point symmetry of the holosymmetric pattern, i.e. $n_j r_j = n_h$.

Bicrystals are supposed to be obtained from dichromatic patterns by choosing the orientation and location of an interface plane and locating white bases at white lattice points on one side of the interface and black bases at black sites on the other. Bicrystals are therefore regarded as three-dimensional objects containing a unique plane, the interface, and the adjacent crystals can have different compositions and structures. Depending on the symmetry of a dichromatic pattern and the choice of interface plane there can be two, one or no translation symmetry axes in the interface plane, and colour symmetry groups can be assigned to bicrystals according to the schemes of two sided layers, bands or rosettes (Shubnikov & Koptsik 1974) respectively. The variation of bicrystal point symmetry with relative displacement of the adjacent crystals follows a conservation rule analogous to that for the case of dichromatic patterns.

The symmetry of the physical properties of bicrystals is considered by invoking Neumann's principle. Computer calculations indicate that the relative displacements of adjacent crystals in mechanically stable polymeric and metallic bicrystals are such that bicrystal symmetry is often lower than holosymmetric. The relative position of adjacent crystals in a bicrystal is an important additional degree of freedom compared to a single crystal. For bicrystals which have at least one-dimensional translation symmetry and point symmetry higher than 1, equivalent bicrystal structures can exist corresponding to crystallographically equivalent relative displacements away from a holosymmetric structure. The number of equivalent bicrystals in a set, r_j, depends on the symmetry of these bicrystals and the holosymmetric form, and is given by the rule $r_j = n_h/n_j$. Such equivalent bicrystals have degenerate energy, and it is possible for domains of equivalent structures, separated by special interfacial dislocations, to exist in a physical bicrystal. The Burgers vectors of these dislocations can have very small magnitudes and the dissociation of perfect interfacial dislocations into special dislocations is discussed.

1. Introduction

No general theory is at present available relating the physical properties of interphase or grain boundaries to their structure. The object of the present work is to point out that Neumann's principle applies to bicrystals as well as to single crystals, and to discuss in this context certain physical properties of bicrystals, in particular their interfacial properties. Neumann's principle is a fundamental postulate of crystal physics (see, for example, Nye 1969) and may be stated as follows for bicrystals: the symmetry elements of any physical property of a bicrystal must include the symmetry elements of the point group of the bicrystal. A physical property consists of the relation between certain measurable quantities associated with the bicrystal, for example, the relation between incident and scattered X-ray intensities.

For the present purposes a bicrystal is considered to consist of two semi-infinite crystals separated by a unique plane, the interface. Point symmetry can always be assigned to a bicrystal, but in addition, there may be one- or two-dimensional translation symmetry in the interface. As far as the present authors are aware, no scheme has been specifically designed for classifying the symmetry of bicrystals, although appropriate systems can certainly be found within the diverse

framework of established crystallography. The major part of this work is to identify these latter systems of symmetry classification and to present them so that the space and/or point symmetry of any bicrystal can be readily classified. This scheme is completely general in the sense that the adjacent crystals in a bicrystal of interest may have different structures and compositions. However, to illustrate the development of this scheme we shall consider predominantly bicrystals where the interface is a grain boundary between adjacent cubic crystals; this procedure is especially helpful in studying bicrystals with high symmetry. The notation for symmetry classification used in this work is the international coordinate system (Shubnikov & Koptsik 1974; Neronova & Belov 1961).

Since details of the atomic positions in real bicrystals are not available at present, idealized bicrystals and relaxed structures obtained by computer simulation are considered. In an idealized bicrystal all atoms are located at the lattice sites of their parent crystal, i.e. there is no interfacial strain field, and there is no thermal vibration. The manufacture and symmetry classification of idealized bicrystals are discussed in §§2 and 4 respectively, and the symmetry of computer simulated structures in §4. In several respects the symmetry of the pattern created by the lattices of the two component crystals of a bircystal proves to be valuable, and this is considered in detail in §3.

In §5 the symmetry of interfacial dislocation networks is considered since these can be an intrinsic part of bicrystal structure. Moreover, these dislocations may have special significance with regard to physical properties such as interfacial diffusion.

2. Crystallography of bicrystals

2.1. *Manufacture of idealized bicrystals*

Consider a lattice, designated the 'white' lattice, which remains fixed in orientation and position. A second lattice, designated 'black', has identical lattice parameters but can have any orientation or position relative to the white. The pattern created by the black and white lattices is called a dichromatic pattern and its symmetry depends on both the relative orientation and position of the two component lattices. To manufacture an idealized bicrystal it is necessary (1) to obtain the appropriate dichromatic pattern, (2) to specify the orientation of the boundary plane, and (3) to locate atomic groups at the sites of the white lattice on one side of the boundary and at the sites of the black lattice on the other. There are eight geometrical degrees of freedom involved in this procedure as outlined below.

Let one white lattice site act as an arbitrarily chosen origin, and consider a vector $[hkl]$ (using the coordinate system of the white lattice) which passes through the origin. A dichromatic pattern may be obtained by the operation $\{[hkl]\,\theta\}'$, which means that a lattice originally coincident with the reference white lattice and with the same colour is rotated by an angle θ about $[hkl]$ and subsequently undergoes colour reversal from white to black (as represented by a prime). All possible relative orientations of the black and white lattices can be obtained in this way, and three degrees of geometrical freedom are associated with the specification of $[hkl]$ and θ. The operation $\{[hkl]\,\theta\}'$ confers on the origin site, for example, both black and white colour; such sites are said to be neutrally coloured.

Any displacement of the black lattice relative to the white after the operation $\{[hkl]\,\theta\}'$ can be characterized by the vector $\boldsymbol{t}$, which is the displacement of the black lattice away from the neutral origin position. Thus, any dichromatic pattern can be characterized by specifying the lattice

PHILOSOPHICAL TRANSACTIONS OF THE ROYAL SOCIETY A MATHEMATICAL, PHYSICAL & ENGINEERING SCIENCES

parameters of the white lattice, $[hkl]\,\theta$ and $\boldsymbol{t}$. Three degrees of geometric freedom are associated with the specification of $\boldsymbol{t}$. (It is noted that there may be alternative but crystallographically equivalent formulations $[hkl]\,\theta$, depending on the crystal lattice symmetry (Warrington & Bufalini 1971).) The final two degrees of geometric freedom in manufacturing a bicrystal are associated with the specification of the boundary plane normal $[pqr]$. When an idealized bicrystal is manufactured as described above, the location of a boundary plane with normal $[pqr]$ is not an independent degree of freedom. Although the atomic configuration at a boundary may change as a result of relocation of the boundary plane, identical changes can be obtained with fixed boundary location by appropriate changes of $\boldsymbol{t}$ (Pond 1977).

TABLE 1. SYMMETRY CLASSES OF DICHROMATIC PATTERNS AND BICRYSTALS

(Nomenclature taken from Shubnikov & Koptsik, 1974)

number of non-parallel translation axes	symmetry class	
	dichromatic patterns	bicrystals
0	point groups	two-sided rosettes
1	crystallographic rods	two-sided bands
2	layers	layers
3	space groups	

2.2. *Symmetry classification of dichromatic patterns and bicrystals*

Dichromatic patterns can have translational symmetry in zero, one, two or three dimensions, thereby containing a singular point, line, plane or lattice respectively. The symmetry of patterns with singular points and lattices can be classified respectively by using the conventional systems comprising point groups and space groups (*International tables* 1969). Patterns with one- and two-dimensional translation symmetry can be classified respectively according to the one-dimensional space groups of crystallographic rods and the two-dimensional space groups of layers (Shubnikov & Koptsik 1974). It is noted that when the component crystal lattices have identical lattice parameters and cubic symmetry, two-dimensional translation symmetry in a dichromatic pattern is not posible. One-dimensional cases are possible, e.g. along $[hkl]$ when this is rational, and three-dimensional examples arise when $[hkl]\,\theta$ leads to coincidence site lattices. Thus dichromatic patterns with symmetry classes in the system of layer space groups occur only for non-cubic crystal lattices, or where the component lattices have different lattice parameters or Bravais classes. In the following text, the component lattices of a dichromatic pattern are always taken to be cubic and with identical lattice parameter unless specifically stated to be otherwise.

Bicrystals are three-dimensional objects containing a singular plane, the interface, in which there can be zero-, one- or two-dimensional translation symmetry. Appropriate systems for the classification of such objects are respectively the symmetry classes of two-sided rosettes, two-sided bands and layers. A two-sided rosette is a figure containing a singular plane and at least one singular point. In two-sided bands and layers the singular plane contains respectively a singular, and two non-collinear translation axes. The 'two-sided' nature of these figures refers to the fact that the singular planes need not be polar, i.e. that looking toward the 'front' and 'back' of the plane need not be different. These symmetry classes for dichromatic patterns and bicrystals are summarized in table 1.

3. Dichromatic pattern symmetry

3.1. *Dichromatic patterns with* $\boldsymbol{t} = 0$

There are two distinct types of point symmetry element in dichromatic patterns: (*a*) ordinary symmetry elements and (*b*) colour reversing symmetry elements. The former occur when identical symmetry elements of the black and white lattices are coincident in a dichromatic pattern, e.g. when [*hkl*] is a symmetry axis or when black and white mirror planes or points with inversion symmetry coincide. Such elements are denoted here by using the international symbols, i.e. *m* for mirror plane, etc. Operation of ordinary symmetry elements always relates sites with identical colour. All points on an ordinary symmetry element correspond to coincidences of points in the black and white lattices which do not in general have the same form of internal coordinates but have identical point symmetry higher than 1.

Operation of colour reversing symmetry elements always relates sites of different colour, or neutral sites to neutral, and these symmetry elements are denoted by the prime on the international symbol, e.g. m' for colour-reversing mirror plane. All points on colour reversing symmetry elements correspond to coincidences of points in the black and white lattices which have identical form of internal coordinates. Points with colour reversing inversion symmetry, $\bar{1}'$, do not occur in dichromatic patterns because their existence implies identical orientation and magnitude of the basic translation vectors of the component crystal lattices. Colour reversing rotation axes, u', can only be evenfold, and arise when two ordinary $u/2$ fold rotation axes coincide and θ is $2\pi/u$.

As indicated in § 2.2, it is helpful to categorize dichromatic patterns according to the number of non-collinear translation axes present. A dichromatic pattern with no translational symmetry can be formed, for example, when [*hkl*] is irrational. In such cases only point symmetry can be assigned, although this can be higher than 1; for example when any one of the crystallographically equivalent descriptions [*hkl*] θ is such that $\theta = \pi$ and [*hkl*] is irrational, a colour reversing mirror plane is obtained on (*hkl*) so that the point symmetry of the dichromatic pattern is m'.

When [*hkl*] is rational there must be at least one-dimensional translation symmetry in a dichromatic pattern, i.e. along [*hkl*]. For example, if [*hkl*] is [001], the one-dimensional crystallographic rod space group is $p4/mm'm'$.

As mentioned above, dichromatic patterns formed from misorientated cubic lattices cannot display two-dimensional translation symmetry. This follows because, if there is translation symmetry parallel to [*lmn*] and [*rst*], there must also be translation symmetry parallel to [*lmn*] × [*rst*]. However, dichromatic patterns with two-dimensional symmetry do occur, for example, when hexagonal lattices with identical lattice parameter, *a*, but where the parameters c_w and c_b (where w and b stand for white and black respectively) are such that c_w/c_b is irrational, are misorientated by certain θ about their common [0001]. Two-dimensional translation symmetry is thereby obtained in the basal plane containing the origin, and the two-dimensional layer space group is $p6/m$.

Next we consider dichromatic patterns, formed from misorientated cubic lattices, which have three-dimensional translation symmetry. When [*hkl*] is rational and θ has special values a space lattice of neutral sites, the coincidence site lattice (c.s.l.), is generated (see, for example, Grimmer *et al.* 1974). C.s.l. have Bravais classes which depend on the Bravais class of the component lattices, and [*hkl*]. C.s.l. are often characterized by a parameter, Σ, defined as the ratio of the unit cell volumes of the c.s.l. and white lattice.

(*a*) $\Sigma=3$, P6′/$m'm'm$

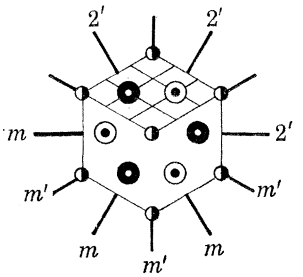

(*b*) $\Sigma=5$, I4/$mm'm'$

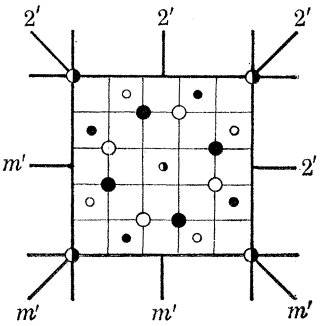

(*c*) $\Sigma=7$, R$\bar{3}m'$

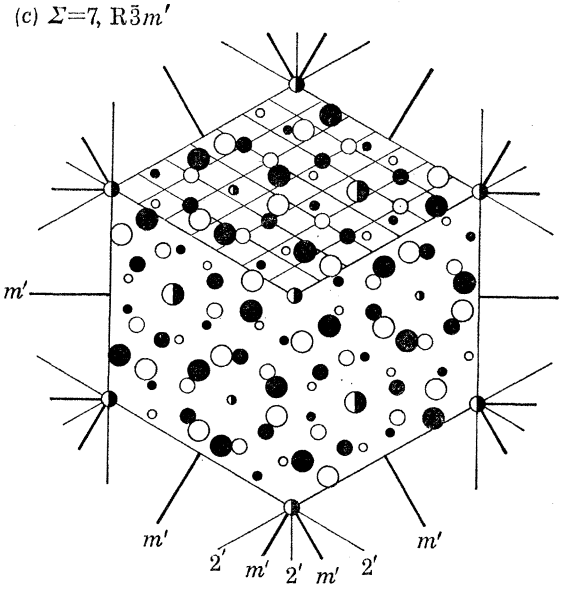

(*d*) $\Sigma=9$, I$m\,m'm'$

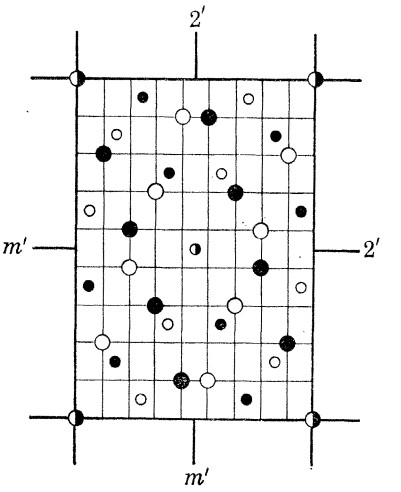

(*e*) $\Sigma=11$, C$m\,m'm'$

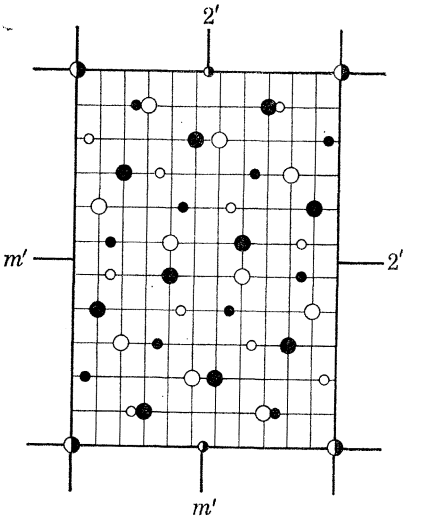

a

FIGURE 1. Projections along [*hkl*] of dichromatic patterns formed by centred cubic lattices: [*hkl*] θ and Σ are as follows: (*a*) [111] 60°, $\Sigma = 3$; (*b*) [001] 36.9°, $\Sigma = 5$; (*c*) [111] 38.21°, $\Sigma = 7$; (*d*) [011] 38.9°, $\Sigma = 9$, (*e*) [011] 50.47°, $\Sigma = 11$. The size of symbols represents the ...ABABA... stacking along [001] and [011] and ...ABCABCAB... along [111].

PHILOSOPHICAL TRANSACTIONS OF THE ROYAL SOCIETY A MATHEMATICAL, PHYSICAL & ENGINEERING SCIENCES

Figure 1 shows the projections along [*hkl*] of five c.s.l. based dichromatic patterns, where [*hkl*] is a symmetry axis of the white lattice which is either face-centred or body-centred cubic. The main symmetry elements are indicated in the figure, but colour reversing mirror glide planes, etc., generated in centred c.s.l. cells have been omitted for clarity. For each of these patterns the three-dimensional space group is also shown in the figure. Inspection of figure 1 shows that the disposition and interaction of colour reversing and ordinary symmetry elements conform to the colour symmetry theorems (see, for example, Loeb 1971). For example, mirror planes in the zone of a colour reversing rotation axis, such as 6′ in figure 1 (*a*), must be disposed alternately *m* and *m*′ (theorem 25).

It is noted that for dichromatic patterns with $[hkl] = \langle 001 \rangle$, and irrespective of the number of non-collinear translation axes present, the point group is always $4/mm'm'$ unless $\theta = \frac{1}{4}n\pi$, where n is an odd integer, when the point group becomes $8'/mmm'$. Similarly, for $[hkl] = \langle 011 \rangle$, the point group is $mm'm'$ for all values of θ except $\frac{1}{2}n\pi$ when the group is $4'/mmm'$, and for $[hkl] = \langle 111 \rangle$ the group is $\bar{3}m'$ unless $\theta = \frac{1}{3}n\pi$ when it becomes $6'/m'mm'$. These special point groups containing colour reversing rotation axes, u', arise when ordinary rotation axes, $u/2$, coincide and $\theta = n2\pi/u$.

3.2. *The variation of dichromatic pattern symmetry with displacement of the black lattice*

When the black lattice is displaced by $\boldsymbol{t}$ away from the neutral origin position the dichromatic pattern changes. Such movements can never modify the number of translation axes present but the space and point symmetry of the dichromatic pattern may be changed. In this section we show first that dichromatic pattern symmetry is invariant for certain displacements, and secondly we discuss the way in which symmetry changes for general displacements.

Consider a dichromatic pattern with $\boldsymbol{t} = 0$ based on a c.s.l.; in such a pattern there are anti-translation vectors, i.e. vectors which join black sites to white. If the black lattice is displaced by an anti-translation vector the original c.s.l. of neutral sites is recreated, but in general has its neutral origin located at a new position. (Anti-translations in a dichromatic pattern do not define an anti-translation lattice (Shubnikov & Koptsik 1974), i.e. a white Bravais lattice with black sites centring the edges, faces or body of the unit cell.) Bollmann (1970) has defined a monochromatic lattice called the d.s.c. lattice associated with any given dichromatic pattern whose primitive translation vectors are equal to the three shortest independent anti-translations in the dichromatic pattern. Bollmann pointed out that displacements of the black lattice (lattice 2 in his terminology) by any vector of the d.s.c. lattice, $\boldsymbol{d}^{\mathrm{sc}}$, reproduce the original pattern but may shift it in space. In the present work we note that the initials d.s.c. conveniently stand for displacements which are symmetry conserving, although this was not Bollmann's original meaning. Thus, the identical dichromatic pattern is obtained by the operations $\{[hkl]\,\theta\}'$, $\boldsymbol{t}$ and $\{[hkl]\,\theta\}'$, $\boldsymbol{t} + \boldsymbol{d}^{\mathrm{sc}}$.

The parameters of a d.s.c. lattice depend on the form of the associated dichromatic pattern; if the dichromatic pattern is aperiodic the primitive d.s.c. vectors have vanishingly small magnitudes. In the cases of patterns with one-dimensional translation symmetry, the primitive d.s.c. vectors are vanishingly small perpendicular to the translation axis, and equal to the basic translation vector along this axis. For patterns based on c.s.l., a d.s.c. lattice has parameters that are related to those of the c.s.l., for example, they are reciprocally related in the case of simple cubic lattices (Grimmer *et al.* 1974). In the case of the dichromatic pattern shown in figure 1 (*b*), for example, the d.s.c. and c.s.l. are both body-centred tetragonal.

It follows from the above discussion that dichromatic pattern symmetry varies periodically with $\boldsymbol{t}$. Thus, when studying the variation of symmetry with $\boldsymbol{t}$ it is only necessary to consider

displacements which fall within the Wigner–Seitz (W.–S.) cell of the associated d.s.c. lattice. Such displacements are referred to as reduced displacements and denoted $\boldsymbol{t}'$. In the case of dichromatic patterns with no translational symmetry the W.–S. cell has zero volume, i.e. the pattern cannot be changed by any displacement although the neutral origin may be shifted by very large distances as a result of displacement. For patterns with one-dimensional translation symmetry the W.–S. cell is a line parallel to the translation axis with magnitude $|\boldsymbol{a}|$ and centred on the neutral origin, where $\boldsymbol{a}$ is the primitive translation vector of the pattern. In the case of patterns based on c.s.l. the W.–S. cell is three-dimensional and has a volume that decreases as Σ increases.

Whereas displacements by $\boldsymbol{d}^{\mathrm{sc}}$ conserve all symmetry in a dichromatic pattern, displacement by other vectors can conserve some of the symmetry elements originally present, while destroying others. Displacements may be classified into two groups, namely:

(i) Displacements which conserve ordinary symmetry elements. An ordinary rotation axis or mirror plane is conserved only by displacements *parallel* to that rotation axis or plane of symmetry respectively. Such displacements ensure that points with identical point symmetry in the black and white lattices remain coincident. Moreover, the location of the symmetry element is invariant.

(ii) Displacements which conserve colour reversing symmetry elements. Rotation axes, u', with $u > 2$, are destroyed by any displacement $\boldsymbol{t}'$. However, axes $2'$ and planes m' are conserved by displacements which are *perpendicular* to these rotation axes and symmetry planes respectively. Thus, for example, in a dichromatic pattern with $\boldsymbol{t}' = 0$ containing a plane m', and therefore an axis $2'$ perpendicular to this, a displacement $\boldsymbol{t}'$ perpendicular to m' conserves this mirror plane but destroys the axis $2'$. The location of the colour reversing mirror is shifted by $\frac{1}{2}\boldsymbol{t}'$. Conversely, if the displacement is parallel to m', and hence perpendicular to $2'$, the former is destroyed and the latter survives, shifted by $\frac{1}{2}\boldsymbol{t}'$. Colour reversing screw diads and mirror glide planes can be created from rational axes $2'$ and planes m' by displacements which have special magnitudes and are parallel to these symmetry elements.

As an illustration of the survival of symmetry elements due to displacement, consider a dichromatic pattern formed initially by the operation $\{[001]\,\theta\}'$, $\boldsymbol{t}' = 0$, i.e. a pattern with one-dimensional translation symmetry parallel to [001]. As described above the rod space group is $p4/mm'm'$; [001] is an ordinary four-fold axis perpendicular to ordinary mirror planes (002), and the colour reversing mirror planes lie in the [001] zone orientated symmetrically between the following four pairs of black and white mirror planes $(100)_{\mathrm{w.b.}}$, $(010)_{\mathrm{w.b.}}$, $(1\bar{1}0)_{\mathrm{w.b.}}$ and $(110)_{\mathrm{w.b.}}$. Since the W.–S. cell of the associated d.s.c. lattice is a line parallel to [001] extending from $-\frac{1}{2}\boldsymbol{a}$ to $+\frac{1}{2}\boldsymbol{a}$ the symmetry of the pattern can only be changed by displacements along this line. Such displacements are parallel to the ordinary fourfold axis, thereby preserving it, but are perpendicular to the ordinary mirror plane, thereby destroying this, and parallel to the colour reversing mirror planes, thereby destroying these. Thus the space group for any translation $\frac{1}{2}\boldsymbol{a} < \boldsymbol{t}' < -\frac{1}{2}\boldsymbol{a}$ is $p4$; for translations $\boldsymbol{t}' = \pm\frac{1}{2}\boldsymbol{a}$, colour reversing mirror glide planes are formed and the space group is $p4/ma'a'$.

3.3. *Equivalent dichromatic patterns*

Whenever a dichromatic pattern with $\boldsymbol{t}' = 0$ contains both translation symmetry and point symmetry higher than 1, there exists a set of dichromatic patterns, obtained from the initial pattern by displacements of the black lattice, which are related by the symmetry elements of the initial pattern. The members of such a set are said to be equivalent patterns, and the translations $\boldsymbol{t}'$ characterizing these are also related by the symmetry elements of the pattern with $\boldsymbol{t}' = 0$. An

illustrative method for describing this property is first to construct the W.–S. cell of the d.s.c. lattice associated with a given dichromatic pattern, and to superimpose on this the point symmetry elements of the dichromatic pattern with $\boldsymbol{t}' = 0$. Figure 2 shows the $[hkl]$ projections of such constructions for the c.s.l. based dichromatic patterns illustrated in figure 1. These constructions have two useful properties:

(i) the numerical point symmetry at a position located by $\boldsymbol{t}'$ in such cells is identical to that of the corresponding dichromatic pattern.

(ii) the number of equivalent dichromatic patterns in a set is equal to the number of points equivalent to $\boldsymbol{t}'$ in the cell.

Consider property (i) (see figure 2): the vectors $\boldsymbol{b}_1$ and $\boldsymbol{b}_2$ are the primitive translation vectors, which are perpendicular to $[hkl]$, of the d.s.c. lattices. Consider the W.–S. cell shown in figure 2 (b): for the $\Sigma = 5$ system with an f.c.c. white lattice (figure 1 (b)) $\boldsymbol{b}_1 = \frac{1}{10}a[310]$, $\boldsymbol{b}_2 = \frac{1}{10}a[1\bar{3}0]$

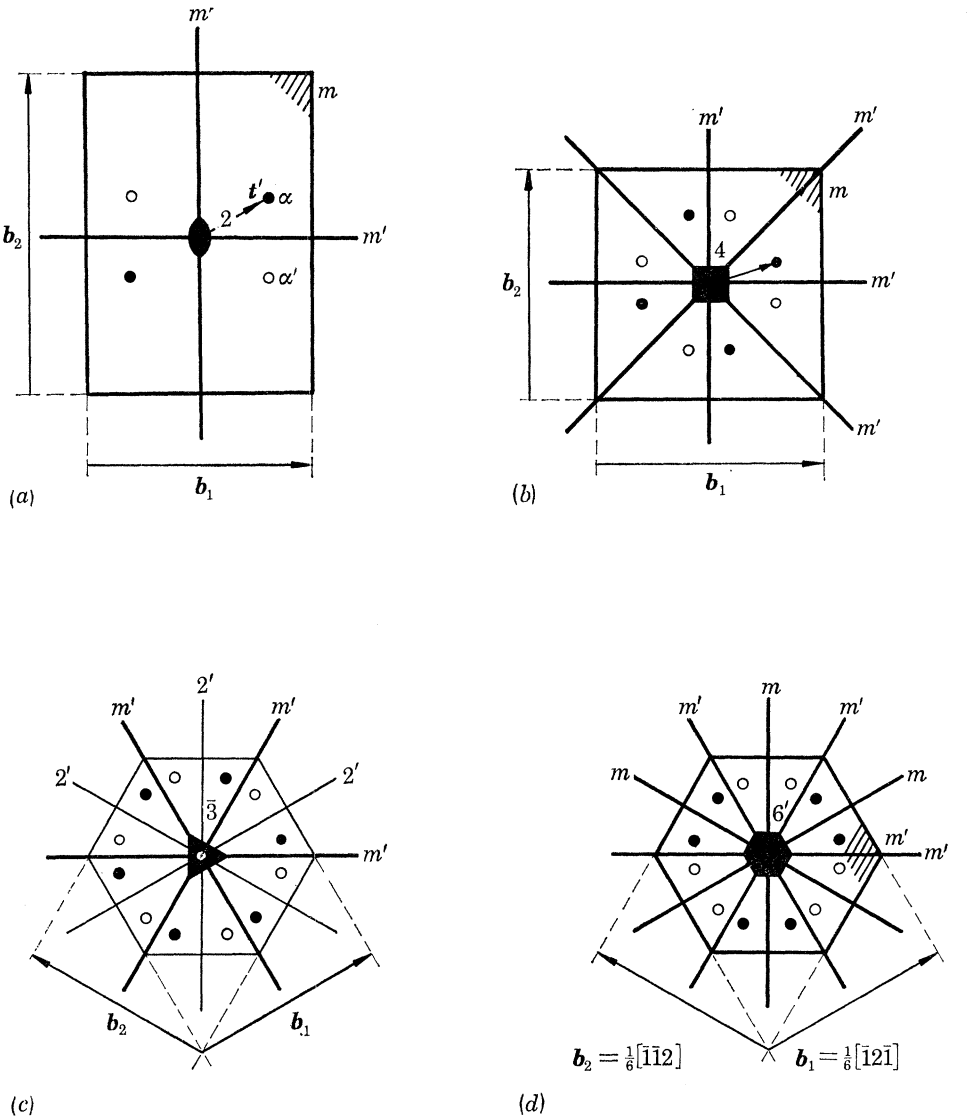

FIGURE 2. Projections along $[hkl]$ of Wigner–Seitz cells of the d.s.c. lattices associated with the c.s.l. based dichromatic patterns shown in figure 1: (a) $[hkl] = \langle 011 \rangle$, (b) $[hkl] = \langle 001 \rangle$, (c) $[hkl] = \langle 111 \rangle$, (d) $[hkl] = \langle 111 \rangle$, $\Sigma = 3$. All displacements shown are perpendicular to $[hkl]$.

([hkl] θ is [001] 36.9°). Figure 3 shows the dichromatic patterns corresponding to $\boldsymbol{t}' = \frac{1}{2}(\boldsymbol{b}_1 - \boldsymbol{b}_2)$, $\frac{1}{2}\boldsymbol{b}_2$, $-x\boldsymbol{b}_1$ and $x(-\boldsymbol{b}_1 + \boldsymbol{b}_2)$ which have point symmetries $4/mm'm'$, $mm'm'$, mm' and mm' respectively. It is clear that the points located by $\boldsymbol{t}'$ in the W.–S. cell, figure 2 (b), have identical point symmetries to the corresponding dichromatic patterns. (It is interesting to note, for example, that the point symmetry of the dichromatic pattern with $\boldsymbol{t}' = 0$ is $4/mm'm'$ which is isomorphous with that of the pattern where $\boldsymbol{t}' = \frac{1}{2}(\boldsymbol{b}_1 - \boldsymbol{b}_2)$; the corresponding space groups are $\mathrm{I}\,4/mm'm'$ and $\mathrm{I}\,4/mc'm'$ respectively.) However, for certain displacements it is the numerical expressions

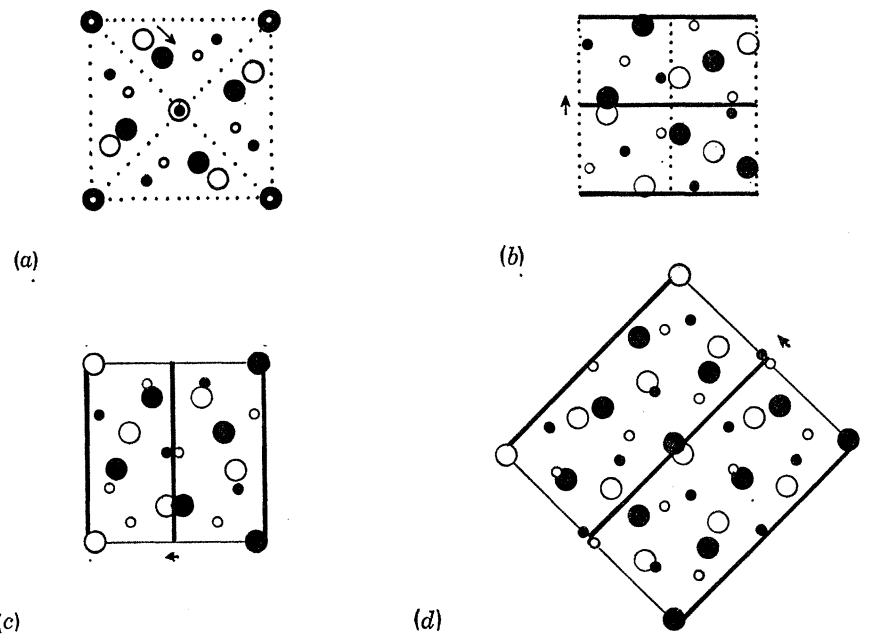

FIGURE 3. [001] projection of $\Sigma = 5$ dichromatic patterns, ([hkl] θ = [001] 36.9°) with $\boldsymbol{t}' \neq 0$; $\boldsymbol{t}'$ is indicated by an arrow in each case and has the following form (a) $\frac{1}{2}(\boldsymbol{b}_1 - \boldsymbol{b}_2)$, ($b$) $\frac{1}{2}\boldsymbol{b}_2$, ($c$) $-x\boldsymbol{b}_1$, (d) $x(\boldsymbol{b}_2 - \boldsymbol{b}_1)$, where $x < \frac{1}{2}$. The space groups for these patterns are given in table 2 (i). These diagrams can also be regarded as [001] projections of twist bicrystals (§4.3), where the white bases are above the interface and the black below. Note that the interface plane is located midway between a plane of small white bases and large black bases. It follows for example that a 2′ axis in the interface plane must relate small bases to large ones of opposite colour.

of the point symmetries that are identical, rather than the symmetry elements themselves. The symmetry elements of a dichromatic pattern are expressed numerically in the following way; $m = 2$, u-fold rotation $= u$. Thus, for example, the numerical expression, designated n, of the point group $3m$ is $n = 6$ and $4/mmm$ is $n = 16$. The latter example illustrates that only the generating symmetry elements need be considered in enumerating n; an alternative definition of n is the multiplicity of general points, irrespective of colour, in the point group in question. An example of equal numerical point symmetry is obtained for a displacement xxz in figure 2 (b); the point symmetry in the W.–S. cell is m' but the symmetry of the corresponding dichromatic pattern is 2′ as shown in table 2(i).

Now consider the second property; associated with a point located by $\boldsymbol{t}'$ in a W.–S. cell there are $(r-1)$ additional points equivalent to the first and obtained by operating the point symmetry elements of the dichromatic pattern (with $\boldsymbol{t}' = 0$). r is the rank of the equipoint located by $\boldsymbol{t}'$. For example, in figure 2 (a) let the dichromatic pattern characterized by $\boldsymbol{t}'$ be designated α. Since $\boldsymbol{t}'$

TABLE 2. VARIATION OF DICHROMATIC PATTERN SYMMETRY WITH RELATIVE DISPLACEMENT $\boldsymbol{t}'$

(The coordinate system for specifying $\boldsymbol{t}'$ is as follows: the origin is taken to be the centre of the Wigner–Seitz cell of the associated d.s.c. lattice, x is parallel to $\boldsymbol{b}_1$, y to $\boldsymbol{b}_2$ and z to $\boldsymbol{b}_1 \times \boldsymbol{b}_2$ (see figure 2).)

fractional coordinates of equivalent displacements $\boldsymbol{t}'$	rank	point symmetry	space symmetry	space group number: international tables	space group number: Shubnikov tables
(i) *C.s.l.-based dichromatic pattern symmetry with* $[hkl] = \langle 001 \rangle$. (f.c.c. or b.c.c. crystal lattices)					
0 0 0	1	$4/mm'm'$	I $4/mm'm'$	139	537
$\frac{1}{2}$ $\frac{1}{2}$ 0	1	$4/mm'm'$	I $4/mc'm'$	140	547
$\frac{1}{2}$ 0 0 0 $\frac{1}{2}$ 0	2	$mm'm'$	I $mm'a'$	74	559
0 0 z 0 0 $\bar{z}$	2	$42'2'$	I $42'2'$	97	154
x 0 0 0 x 0	4	mm'	I $m'm2'$	44	231
$\bar{x}$ 0 0 0 $\bar{x}$ 0					
x x 0 $\bar{x}$ x 0	4	mm'	F $m'm2'$	42	221
x $\bar{x}$ 0 $\bar{x}$ $\bar{x}$ 0					
x 0 z 0 x z	8	$2'$	C $2'$	5	15
$\bar{x}$ 0 z 0 $\bar{x}$ z					
x 0 $\bar{z}$ 0 x $\bar{z}$					
$\bar{x}$ 0 $\bar{z}$ 0 $\bar{x}$ $\bar{z}$					
x x z $\bar{x}$ x z	8	$2'$	C $2'$	5	15
x $\bar{x}$ z $\bar{x}$ $\bar{x}$ z					
x x $\bar{z}$ $\bar{x}$ x z					
x $\bar{x}$ $\bar{z}$ $\bar{x}$ $\bar{x}$ $\bar{z}$					
x y 0 y x 0	8	m	C m	8	32
x $\bar{y}$ 0 y $\bar{x}$ 0					
$\bar{x}$ $\bar{y}$ 0 $\bar{y}$ $\bar{x}$ 0					
$\bar{x}$ y 0 $\bar{y}$ x 0					
x y z $\bar{x}$ y z	16	1	P 1	1	1
x $\bar{y}$ z $\bar{x}$ $\bar{y}$ z					
y x z $\bar{y}$ x z					
y $\bar{x}$ z $\bar{y}$ $\bar{x}$ z					
x y $\bar{z}$ $\bar{x}$ y $\bar{z}$					
x $\bar{y}$ $\bar{z}$ $\bar{x}$ $\bar{y}$ $\bar{z}$					
y x $\bar{z}$ $\bar{y}$ x $\bar{z}$					
y $\bar{x}$ $\bar{z}$ $\bar{y}$ $\bar{x}$ $\bar{z}$					
(ii) *C.s.l.-based dichromatic pattern symmetry with* $[hkl] = \langle 011 \rangle$ ($\Sigma = 9$ type c.s.l., f.c.c. crystal lattices)					
0 0 0 —	1	$m'm'm$	I $m'm'm$	71	536
$\frac{1}{2}$ 0 0 —	1	$m'mm'$	I $m'ma'$	74	559
0 $\frac{1}{2}$ 0 —	1	$m'mm'$	I $m'ma'$	74	559
x 0 0 $\bar{x}$ 0 0	2	$m'm2'$	I $m'm2'$	44	231
0 y 0 0 $\bar{y}$ 0	2	$m'm2'$	I $m'm2'$	44	231
0 0 z 0 0 $\bar{z}$	2	$2'2'2$	I $2'2'2$	23	51
x 0 z x 0 $\bar{z}$	4	$2'$	C $2'$	5	15
$\bar{x}$ 0 z $\bar{x}$ 0 $\bar{z}$					
0 y z 0 y $\bar{z}$	4	$2'$	C $2'$	5	15
0 $\bar{y}$ z 0 $\bar{y}$ $\bar{z}$					
x y 0 $\bar{x}$ y 0	4	m	C m	8	32
x $\bar{y}$ 0 $\bar{x}$ $\bar{y}$ 0					
x y z $\bar{x}$ y z	8	1	P 1	1	1
x $\bar{y}$ z $\bar{x}$ $\bar{y}$ z					
x y $\bar{z}$ $\bar{x}$ y $\bar{z}$					
x $\bar{y}$ $\bar{z}$ $\bar{x}$ $\bar{y}$ $\bar{z}$					
(iii) *C.s.l. based dichromatic pattern symmetry with* $[hkl] = \langle 111 \rangle$ ($\Sigma = 7$ type, f.c.c. or b.c.c. crystal lattices)†					
0 0 0	1	$\bar{3}m'$	R $\bar{3}m'$	166	101
0 0 z	2	$32'$	R $32'$	155	47
$\frac{1}{3}$ $\frac{1}{3}$ 0	2	$32'$	R $32'$	155	47
$\frac{1}{2}$ 0 0	3	$2'/m'$	C $2'/m'$	12	62
x 0 0	6	m'	C m'	8	34
x x z	6	$2'$	C $2'$	5	15
x y z	12	1	P 1	1	1

† Only one example of fractional coordinates is given in each case.

in this case is perpendicular to $[hkl]$, $r = 4$ and the point symmetry of the four corresponding dichromatic patterns is m. These four patterns are referred to as equivalent patterns, and the pattern labelled α' in figure 2 (*a*), for example, can be obtained from α by operation of a colour reversing mirror perpendicular to $\boldsymbol{b}_2$, i.e. in the same way that the characteristic displacement for α' is obtained from $\boldsymbol{t}'$. Filled and unfilled circles in figure 2 represent a colour reversed relation between dichromatic patterns in an equivalent set. In figure 2 (*b*), for example, the dichromatic patterns corresponding to the four open circles are all congruent, and related by colour reversing mirror symmetry to the four congruent patterns represented by the filled circles.

This property of equivalent sets of points in a W.–S. cell can be expressed numerically. For a dichromatic pattern obtained by the operation $\{[hkl]\,\theta\}'$ each set of r equivalent patterns will have numerical symmetry n such that the product rn is invariant with $\boldsymbol{t}'$. For example, in the case illustrated in figure 2 (*a*), $r = 4$ and $n = 2$. Note that for $\boldsymbol{t}' = 0$ the pattern has $r = 1$ and $n = 8$, i.e. point symmetry $mm'm'$. A pattern corresponding to the most general displacement, e.g. $\boldsymbol{t}'$ (figure 2 (*a*)) plus a component parallel to $[hkl]$ so that the point symmetry of the corresponding dichromatic pattern is 1, will have $r = 8$ and $n = 1$. Table 2 (i)–(iii) documents the variation of dichromatic pattern symmetry with $\boldsymbol{t}'$ for examples of the cubic system where $[hkl]$ is $\langle 100\rangle$, $\langle 110\rangle$ and $\langle 111\rangle$.

4. Symmetry of bicrystals

4.1. *Orientation of symmetry elements in bicrystals*

To manufacture an idealized bicrystal from a dichromatic pattern it is necessary to do two things. First, the interface plane, (pqr) must be selected; the interface is considered to be a geometrical dividing plane separating the black lattice sites from the white. Secondly, an atomic group, or basis, must be located at each lattice site; let a black basis be associated with each black lattice site below the interface plane and a white basis with each site above. A basis may be a single atom, a group of atoms, or a molecule; in a given bicrystal black and white bases may be different, in which case no colour reversing symmetry elements exist, or identical as in the case of grain boundaries in simple metals. In bicrystals where black and white bases are physically identical, the justification for retaining the concept of colour reversing symmetry elements is that this simplifies considerations of, for example, the retention or destruction of bicrystal symmetry elements as a result of relative displacement of the two crystals. The orientations of point symmetry elements in a bicrystal are restricted by the orientation of the interface plane as follows:

(i) ordinary rotation axes and mirror planes must be perpendicular to the interface because they relate bases with identical colour;

(ii) colour reversing rotation axes can only be twofold; these, and also colour reversing mirror planes can only exist parallel to an interface since they relate bases of different colour. (Colour reversing roto–inversion axes cannot exist in bicrystals because these require that the basic crystal translations are identical on either side of the interface.)

The presence and disposition of translation symmetry elements in a bicrystal is also restricted by the orientation of the interface. In the case of bicrystals manufactured from dichromatic patterns with one-dimensional translation symmetry, there will be no translation symmetry in a bicrystal unless the interface plane is parallel to the translation axis. For bicrystals manufactured from c.s.l. based dichromatic patterns, rational interface planes must contain two non-collinear translation axes.

PHILOSOPHICAL TRANSACTIONS OF THE ROYAL SOCIETY A MATHEMATICAL, PHYSICAL & ENGINEERING SCIENCES

Compound symmetry elements have orientational restrictions as for point symmetry elements; e.g. colour reversing mirror glide planes can only exist parallel to an interface.

4.2. *Bicrystal symmetry classification*

The point group of a bicrystal must be a subgroup of that for the dichromatic pattern from which it was manufactured. The symmetry elements present in a bicrystal will depend on the orientation of the interface. This is illustrated by table 3 which lists the layer space groups of bicrystals manufactured from the $\Sigma = 5$ c.s.l. based dichromatic pattern with $\boldsymbol{t}' = 0$ (figure 1*b*). Bicrystals with interfaces parallel to any other rational plane will have the layer space group $p1$, i.e. two non-collinear translation axes but no point symmetry elements. The point symmetry of the dichromatic patterns is $4/mm'm'$, but it is seen from table 3 that it is not possible to manufacture bicrystals with point symmetries belonging to all subgroups of $4/mm'm'$, e.g. bicrystals with point symmetry $4/m$ and $4m'm'$ cannot be obtained. This is a consequence of the restriction of bicrystal symmetry elements imposed by a choice of interface plane.

TABLE 3. HOLOSYMMETRIC BICRYSTAL STRUCTURES BASED ON THE $\Sigma = 5$ DICHROMATIC PATTERN WITH $\boldsymbol{t}' = 0$.

interface plane		layer space group of holosymmetric bicrystal
f.c.c. indexing	c.s.l. indexing	
(001)	$(001)_c$	$p42_12'$
(310), (1$\bar{3}$0)	$(100)_c$, $(010)_c$	$p2'mm'$
(2$\bar{1}$0), (120)	$(110)_c$, (1$\bar{1}$0)$_c$	$p2'mm'$
(lm0)	$(rs0)_c$	$p1m1$
(l, $\bar{3}l$, 0), (3l, $\bar{l}$, 0)	$(0rs)_c$, $(r0s)_c$	$p12'1$
(l, $\bar{2}l$, 0), (2l, $\bar{l}$, 0)	$(r\bar{r}0)_c$, $(rr0)_c$	$p12'1$

The component crystals are f.c.c.; the faces of the c.s.l. unit cell have indices (310), ($\bar{1}$30), (001) and $(100)_c$, $(010)_c$, $(001)_c$, where brackets without subscripts refer to the coordinate system of the white crystal, and those with subscript c refer to the c.s.l. $l \neq m$ and $r \neq s$ but all are integers.

The space groups listed in table 3 correspond to the holosymmetric bicrystals for each of the interface orientations chosen. It is always possible to reduce the symmetry of these bicrystals by relative displacement of the two crystals. As an illustration consider the bicrystal formed from the $\Sigma = 5$ c.s.l. with $\boldsymbol{t}' = 0$ (figure 1*b*) where the interface plane is (310) (i.e. parallel to the $(100)_c$ edge face of the c.s.l. unit cell). Table 3 indicates that the holosymmetric bicrystal structure has point symmetry $2'mm'$. In fact there are six structures, with different relative displacements, that have symmetry isomorphous with $2'mm'$ as illustrated in figure 4 (*a*)–(*f*). The symmetry elements retained in bicrystals as a result of relative displacements follow precisely the same rules as for symmetry elements in dichromatic patterns (section 3.2). Bicrystals with point symmetry in the subgroup classes of $2'mm'$, i.e. m, $2'$ and 1, can be obtained by appropriate displacements parallel to the interface as illustrated in figure 4 (*g*)–(*i*).

The (310) bicrystal discussed above is an example of a tilt bicrystal, i.e. one where the rotation axis [*hkl*] is parallel to the interface. Figures 1 and 3, which were considered in § 3, can be regarded as [*hkl*] projections of bicrystals where the interface is parallel to the page and the white bases are above the page and the black below. (Note that neutral sites must become either black or white bases.) Since [*hkl*] is perpendicular to the interfaces in all cases, these are examples of twist

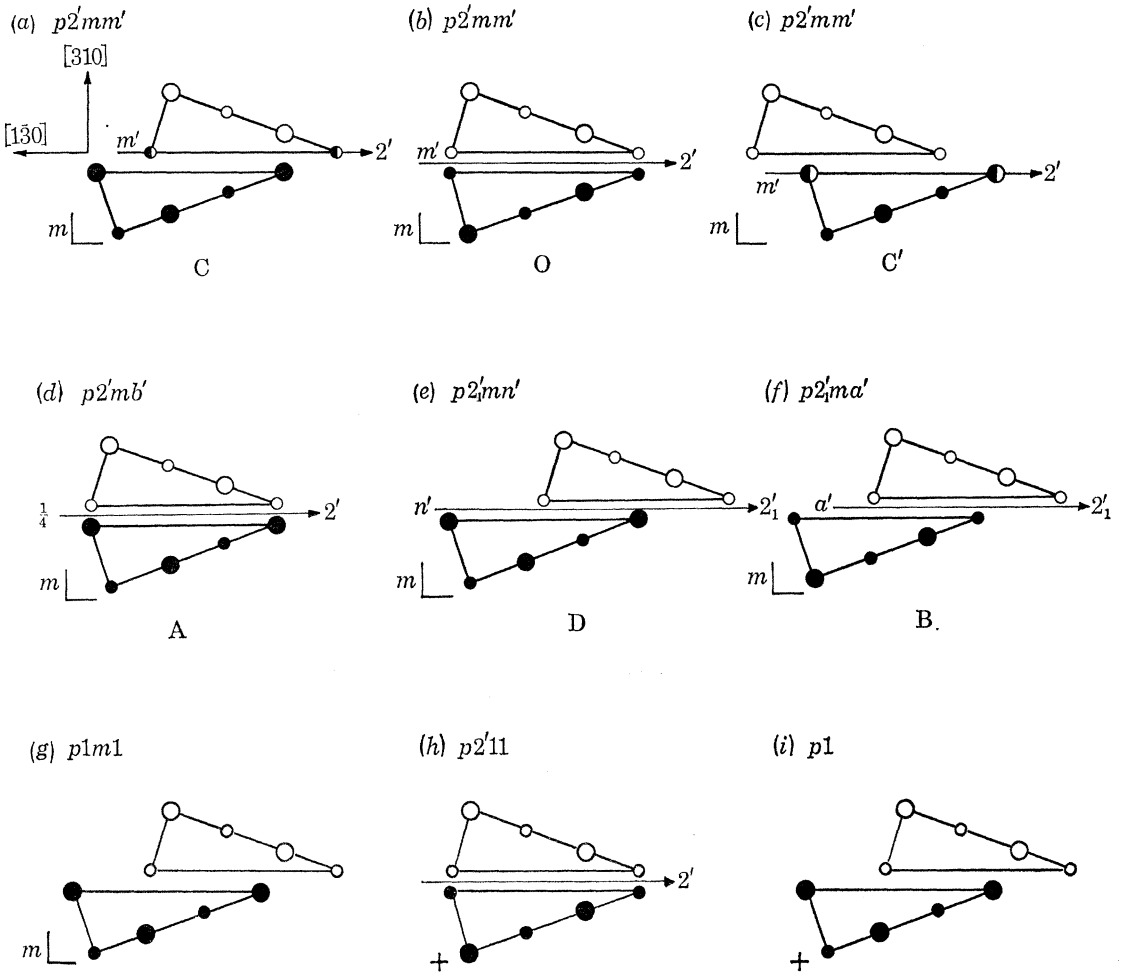

FIGURE 4. Symmetry elements of the (310) $\Sigma = 5$ bicrystal (f.c.c. crystals). The projection direction is [001] and one repeat of the atomic structure immediately adjacent to the interface is shown to represent each bicrystal. The direction of projection corresponds to $[001]_c$ and the b axis of the coordinate system used to define the layer space groups. The symbols '+' indicate that the black crystal has been displaced out of the page.

TABLE 4. VARIATION OF LAYER SPACE GROUPS WITH RELATIVE DISPLACEMENT $\boldsymbol{p}_i'$ FOR (001) TWIST BICRYSTALS BASED ON THE $\Sigma = 5$ DICHROMATIC PATTERN

fractional coordinates of equivalent relative displacements $\boldsymbol{p}_i'$	illustration figure	layer space group	rank
$\mathbf{0}$	3 (*a*)	$p42'2'$	1
$\frac{1}{2}(\boldsymbol{b}_1+\boldsymbol{b}_2)$	1 (*b*)	$p42_1'2'$	1
$\frac{1}{2}\boldsymbol{b}_1$, $\frac{1}{2}\boldsymbol{b}_2$	3 (*b*)	$p2_1'2'2$	2
$x\boldsymbol{b}_1$, $x\boldsymbol{b}_2$	3 (*c*)	$p12'1$	4
$-x\boldsymbol{b}_1$, $-x\boldsymbol{b}_2$			
$x(\boldsymbol{b}_1+\boldsymbol{b}_2)$, $x(\boldsymbol{b}_1-\boldsymbol{b}_2)$	3 (*d*)	$p12'1$	4
$-x(\boldsymbol{b}_1+\boldsymbol{b}_2)$, $-x(\boldsymbol{b}_1-\boldsymbol{b}_2)$			
$x\boldsymbol{b}_1+y\boldsymbol{b}_2$, $x\boldsymbol{b}_1-y\boldsymbol{b}_2$		$p1$	8
$-x\boldsymbol{b}_1+y\boldsymbol{b}_2$, $-x\boldsymbol{b}_1-y\boldsymbol{b}_2$			
$y\boldsymbol{b}_1+x\boldsymbol{b}_2$, $y\boldsymbol{b}_1-x\boldsymbol{b}_2$			
$-y\boldsymbol{b}_1+x\boldsymbol{b}_2$, $-y\boldsymbol{b}_1-x\boldsymbol{b}_2$			

boundaries. The layer space groups and relative displacements for these twist boundary structures are given in table 4, and are discussed further later in this section.

4.3. *Equivalent bicrystal structures*

As for the case for dichromatic patterns, sets of equivalent bicrystal structures exist whenever the holosymmetric bicrystal contains both translation symmetry and point symmetry higher than 1. Equivalent bicrystals have degenerate energy, and structures related by the point symmetry elements of the holosymmetric structure. The relative displacements of equivalent structures are also related by these symmetry elements.

To illustrate the existence of equivalent bicrystal structures it is helpful to construct a W.–S. cell for relative displacements. Once the plane of a bicrystal interface has been chosen, all possible idealized bicrystal structures can be produced by relative displacements parallel to the interface. It is therefore convenient to use a W.–S. cell which is planar and parallel to the interface.

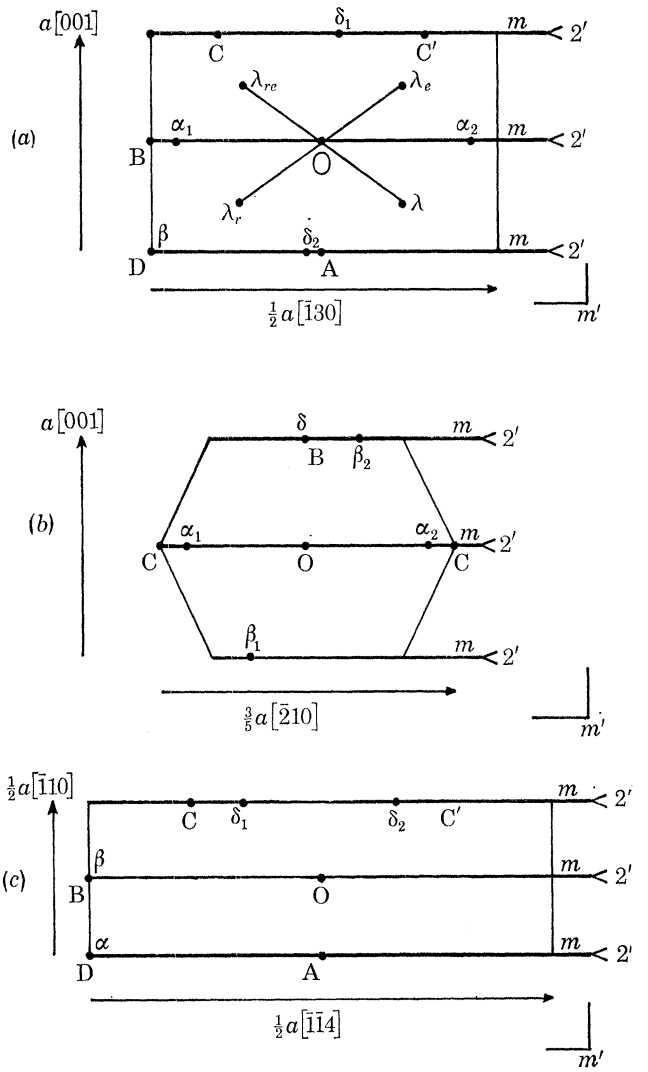

FIGURE 5. In-plane Wigner–Seitz cells for tilt boundaries in aluminium (*a*) (310) $\Sigma = 5$, (*b*) (120) $\Sigma = 5$, (*c*) (221) $\Sigma = 9$.

Displacements which fall within such in-plane W.–S. cells are termed reduced in-plane displacements and designated $\boldsymbol{p}'_i$. In the case of bicrystals with one-dimensional translation symmetry in the interface the in-plane W.–S. cell is a line parallel to the translation axis in the interface and is identical to that used for dichromatic patterns with one-dimensional translation symmetry. For bicrystals with two non-collinear translation axes, the most convenient in-plane W.–S. cell has been described in detail by Pond (1977). This comprises a cell parallel to the interface bounded by $\boldsymbol{d}^{sc}$ vectors which are not primitive for tilt boundaries. Figure 5 (*a*) shows the cell for the (310), $\Sigma = 5$ bicrystal, where the adjacent crystals are f.c.c., illustrated in figure 4; in this type of interface the in-plane cell is simply the W.–S. cell of the white lattice vectors in the lowermost (620) atomic plane of that crystal. Any idealized bicrystal can be represented by a point in this cell; such points simply correspond to the projection onto the W.–S. cell of a site in the uppermost atomic layer of the black crystal. We define a reference structure to be that structure represented by the point O, at the centre of the cell. In the case of the (310) bicrystal the reference structure is designated O in figure 4 (*b*) and is holosymmetric for this interface plane. Other (310) structures with high symmetry are designated A, B, D in figures 4 and 5 (*a*), and the classical coincidence structure is designated C and C′. We note that in this latter structure the unique plane containing the symmetry elements also contains neutral bases. This contrasts with the other structures shown in figure 4 which contain no bases in the geometrical interface plane.

Once an in-plane W.–S. cell has been obtained, the number of structures in an equivalent set can be found by superimposing on the cell the point symmetry elements of the reference structure. The number of structures equivalent to one characterized by $\boldsymbol{p}'_i$ is simply the same as the number of points equivalent to the point $\boldsymbol{p}'_i$ in the W.–S. cell. For example, consider the (310), $\Sigma = 5$ structure designated λ in figure 5 (*a*). There are three additional equivalent structures obtained from λ as follows:

λ_e Operation of the ordinary mirror plane (002).

λ_r Operation of 2′ (parallel to [$\bar{1}$30]); note that this operation does not produce λ_e from λ, as might be expected on first inspection, because 2′ is a colour reversing symmetry operation and the structures are characterized by the displacement of the black crystal (always the lower) away from the reference position.

λ_{re} Obtained from λ by the combination of operations *m* and 2′.

These four and the reference structure are illustrated schematically in figure 6. It is clear that if the white and black bases are identical, the colour reversed pairs of structures, e.g. λ and λ_r, are physically identical and the pairs related by ordinary mirror symmetry, e.g. λ and λ_e, are physical enantiomorphs.

The point symmetry of a bicrystal can be established from the position of its representation point in the in-plane W.–S. cell. For example, consider again figure 5 (*a*); it is clear that the bicrystal λ has no point symmetry because the displacement from the reference structure, O, is such as to destroy all of these initial symmetry elements (i.e. the displacement has a component parallel to 2′ and *m*′, thereby destroying these, and perpendicular to *m*, thereby destroying this). In addition, the number of equivalent structures *r*, is given by the rank of the representation point, and the product of the numerical symmetry and the rank of a structure is invariant. Thus, the product for the four structures λ, λ_e, λ_r and λ_{re} is 1×4. The structures represented by points O, A, B and D are all rank 1 positions with numerical symmetry 4 (see figure 4). Any structure represented by a point on the 2′ axis, (or the edges of the cell parallel to this) but excluding the rank 1 points, has rank 2 and symmetry *m*. Any structure represented by a point on OA, but

excluding points O and A, will have symmetry 2′ and rank 2. Special comment is required for the coincidence structures C and C′ (figures 4*a*, *c*, and 5*a*). According to figure 4 these structures have symmetry 2′*mm*′, which is inconsistent with the procedure outlined above, which would suggest symmetry *m*. This arises because one layer of bases in figure 4(*a*) and (*c*) have been coloured neutrally; if this layer were either black or white the resultant symmetry would be *m* as required. However, it should be noted that in a real bicrystal with black bases identical to white a structure with symmetry 2*mm* (dropping the colour reversing superscripts) is obtained for this special relative displacement.

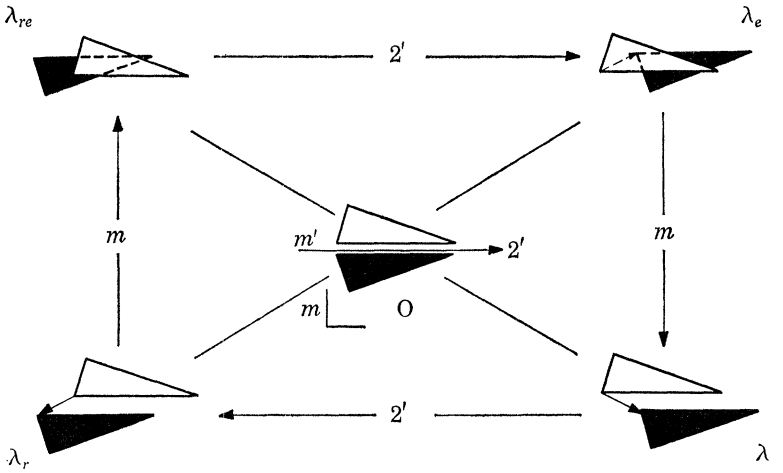

FIGURE 6. Schematic representation of four equivalent bicrystal structures for the (310) $\Sigma = 5$ bicrystal. The holosymmetric reference structure, O, and the symmetry elements relating the equivalent structures are also shown.

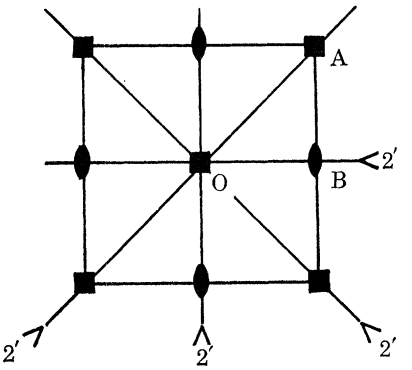

FIGURE 7. In-plane Wigner–Seitz cell for (001) twist boundary structures with the symmetry elements of the holosymmetric bicrystal superimposed.

Consider next some examples of twist bicrystals as depicted in figures 1 and 3. In particular, consider the $\Sigma = 5$ bicrystal, figure 1(*b*) and 3, which has $[hkl] = [001]$ and $(pqr) = (001)$. The in-plane W.–S. cell for such a bicrystal is bounded by primitive $\boldsymbol{d}^{sc}$ (Pond 1979), as is shown in figure 7. The most convenient choice of reference structure is that manufactured from the dichromatic pattern with $\boldsymbol{t}' = \frac{1}{2}(\boldsymbol{b}_1 + \boldsymbol{b}_2)$, which has the layer space group $p42'2'$ (figure 3*a*). If the symmetry elements of this holosymmetric structure are superimposed on the W.–S. cell the structures equivalent to any given structure can be found. Apart from the reference structure, O, represented by the point at the centre of the in-plane W.–S. cell, there is only one other rank 1 position. This is the corner of the cell, point A (figure 7), and represents the structure

manufactured from the coincidence dichromatic pattern (i.e. $\boldsymbol{t}' = 0$, figure 1*b*), for which the in-plane displacement relative to the reference structure, $\boldsymbol{p}_1'$, is $\frac{1}{2}(\boldsymbol{b}_1 + \boldsymbol{b}_2)$ and the layer space group $p42_1'2'$. The point B corresponds to a rank 2 position and leads to the space group $p2_1'2'2$. Points on the lines OB and OA correspond to structures with the layer space group $p12'1$ and have rank 4. For the most general structure, $\boldsymbol{p}_i' = x\boldsymbol{b}_1 + y\boldsymbol{b}_2$, where x and y are fractional and unequal, the layer space group is $p1$ and there are eight equivalent structures. These (001) twist structures are summarized in table 4.

It is clear that the product $n_j r_j$, where n_j is the numerical point symmetry of a bicrystal with rank r_j, is invariant for a given bicrystal and is equal to n_h, the numerical point symmetry of the holosymmetric form of that bicrystal. This conservation rule shows the importance of the holosymmetric form, even if this bicrystal does not exist in nature. We note that the conservation rule is obeyed even in the case of the coincidence tilt grain boundary structures, C and C', cited above as a special case. These structures have numerical point symmetry $n_j = 4$, but since C and C' are physically indistinguishable their rank is 1. Thus the product $n_j r_j$ remains equal to the numerical symmetry of the holosymmetric reference structure.

The equivalent bicrystal structures described in this work have been obtained by symmetrically related rigid displacements of the lower crystal away from a reference structure, and local atomic relaxation has not been considered. Local atomic relaxation may occur in such a way as to leave unchanged, decrease or increase the symmetry of a given structure. However, the conservation rule is still obeyed whichever type of relaxation occurs. If the symmetry is decreased the rank increases correspondingly, and this will be reported in more detail in a later publication.

4.4. *Symmetry of relaxed computer simulated grain boundaries*

By using high speed computers it is possible to simulate an idealized bicrystal and allow its constituent atoms to move according to the resultant forces which act on them. In the work of Smith *et al.* (1977), Pond & Vitek (1977) and Pond *et al.* (1979), for example, tilt boundaries in aluminium with $[hkl] = \langle 001 \rangle$ and $\langle 011 \rangle$ have been studied, and it was found that relaxation occurs both by relative displacement of the two crystals and by local movement of individual atoms. Although it was possible for local atom movements to destroy bicrystal symmetry elements present following rigid relative displacements of the crystals, this was not found to occur in mechanically stable structures. In other words, although local atom movements did occur in addition to relative displacements, the former were always such as to conserve the symmetry elements expected according to the position of the representation point in the in-plane W.–S. cell. This occurred in spite of algorithms constructed to avoid restriction of atom movements due to imposed symmetries (see §5) and relaxation procedures in which relative displacement and local movements could occur simultaneously.

Figure 5 (*a*)–(*c*) show the in-plane W.–S. cells for $\Sigma = 5\,(310)$, $\Sigma = 5\,(120)$ and $\Sigma = 9\,(221)$ grain boundaries between f.c.c. crystals. Singular points, O, A, B, D, corresponding to holosymmetric structures are indicated, and the relaxed mechanically stable structures are denoted by lower case Greek letters with grain boundary energy, γ, increasing in the order α, β, δ. Subscripted structures, e.g. α_1, α_2 correspond to equivalent structures. It is particularly noteworthy that many structures retained the ordinary mirror symmetry, m, and that the (310) β, and (221) α and β structures are holosymmetric. We also note that the classical coincidence structure C and C' were not found to be favourable, i.e. low γ, structures. The full details of γ, and relative displacements for these boundaries, have been published (Smith *et al.* 1977; Pond *et al.* 1979). In

all cases there was relaxation perpendicular to the boundary, i.e. decreasing the density of the boundary material, but this does not destroy any of the symmetry elements shown in figure 5.

Twist boundary structures formed between crystals of Cu and Ni with $[hkl] = [001]$ and $(pqr) = (001)$ have been studied by Bristowe & Crocker (1978). They find that, for both types of metal, three stable bicrystals with similar energy exist, corresponding to points O, A and B in figure 7, in the $\Sigma = 5$, 13, 17 and 25 systems. Moreover, in spite of local atomic movements in addition to relative displacements in these relaxed bicrystals all the symmetry elements expected in idealized bicrystals represented by points O, A and B were conserved.

5. Interfacial dislocation networks

5.1. *Burgers vectors of interfacial dislocations*

The term 'interfacial dislocation' is used here to describe special dislocations which exist in interfaces. All grain boundary structures can be considered as arrays of primary, or crystal, dislocations but these may have a formal significance only since they may be very closely spaced. Primary dislocations are excluded from our present considerations. Any structure that contains translation symmetry can be dislocated, and the presence of point symmetry in a structure is immaterial as far as the nature of perfect dislocations is concerned. In this section we shall deal with interfacial dislocations in grain boundaries based on c.s.l. Bollmann (1970) has shown that for such cases the basic translation vectors of the associated d.s.c. lattice are possible Burgers vectors of perfect interfacial dislocations, and he has termed such dislocations secondary dislocations. We note the following very important distinction between secondary and primary dislocations; whereas the Burgers vectors of primary dislocations are the basic translation vectors of the underlying crystal lattice, the Burgers vectors of secondary dislocations are not in general equal to translation vectors which exist in the interface in question. The essential feature of $\boldsymbol{d}^{\mathrm{sc}}$ vectors which qualifies them as secondary dislocation Burgers vectors is that displacements of the black lattice by $\boldsymbol{d}^{\mathrm{sc}}$ recreate the identical dichromatic pattern. Therefore, identical bicrystal structures can be obtained from the dichromatic pattern before and after displacement. However, as noted in § 3, after displacement the origin of the dichromatic pattern may be shifted in space, and as a consequence of this secondary dislocations can have interfacial steps associated with their cores (see for example, Pond 1977). Numerous experimental observations of secondary dislocations have been reported; for example, Balluffi *et al.* (1972). Dislocations have been observed in bicrystals based on dichromatic patterns with one-dimensional translation symmetry (Darby *et al.* 1978), but these are partial dislocations in the sense that their Burgers vectors are parallel to the basic $\boldsymbol{d}^{\mathrm{sc}}$ vector but are only half the magnitude of the latter.

5.2. *Secondary dislocation networks comprising perfect dislocations*

An important function of networks of secondary dislocations is to accommodate small angular deviations from favourable bicrystal structures, such as those known to be based on certain c.s.l. Warrington & Bollmann (1972) showed that such secondary dislocation networks can be treated similarly to subgrain boundaries. The form and symmetry of a network depend on the angular deviation from the c.s.l. misorientation in question, and the plane of the interface. We note that the actual relative displacement at a boundary is irrelevant to the treatment of networks of perfect secondary dislocations provided we assume that only one interface structure, i.e. a rank1 structure, is present.

PHILOSOPHICAL TRANSACTIONS OF THE ROYAL SOCIETY A MATHEMATICAL, PHYSICAL & ENGINEERING SCIENCES

A procedure for predicting the form of secondary dislocation networks has been presented by Bollmann (1970) using the 'O'-lattice method, and this is briefly outlined below. First the b-lattice is constructed; this is the d.s.c. lattice associated with the exact coincidence misorientation. The b-lattice is intersected by the b-subspace which is a plane passing through the origin of the b-lattice perpendicular to the axis of rotation which represents the deviation from the coincidence orientation. Those points of the b-lattice on or in the immediate vicinity of the b-subspace, are connected to form the b-net. The Burgers vectors of $\boldsymbol{d}^{\mathrm{sc}}$ vectors in the b-net are those which can be used to form a secondary dislocation network ensuring that in the network the summation of Burgers vector parallel to the rotation axis of deviation is zero.

To construct the dislocation network from the b-net, tracing paper is placed over a drawing of the b-net and the centres of all the neighbouring polygons of the b-net are connected by lines. This drawing represents a twist dislocation network. To obtain the correct orientation and size, the drawing should be expanded by $1/(2\sin\frac{1}{2}\phi)$ and rotated by $\frac{1}{2}\phi - 90°$, where ϕ is the angular deviation.

The Burgers vector of a drawn dislocation line is that vector in the b-net which has been crossed on drawing the line. The relative orientation of the Burgers vector to the dislocation line is determined by the rotation of the dislocation network with respect to the b-net. The relation between the sign of the Burgers vector and the dislocation line sense is given by the duality relation D4 (Bollmann (1970), p. 123). Finally, the network obtained must be projected perpendicularly onto the interface plane.

As a simple illustration consider a twist grain boundary separating two identical hexagonal crystals where the rotation axis is the common [0001] and θ is close to a value leading to a c.s.l. Thus, the secondary dislocation network is a simple twist network. Figure 8 (*a*) shows the b-net for this bicrystal on the right and the expected dislocation network on the left. The change of scale and orientation are indicated. The dashed network in the b-net of figure 1 (*a*) represents not only the first stage of construction of the network from the b-net but also the in-plane W.–S. cell for this bicrystal.

5.3. *Secondary dislocation networks comprising partial dislocations*

In the previous section we considered an interface having a unique structure. Dislocations in such an interface must be perfect $\boldsymbol{d}^{\mathrm{sc}}$ dislocations. In this section we consider the modifications to dislocation networks when an interface can contain regions with two or more different but equivalent structures. In such bicrystals, dislocations can exist which separate regions of interface with equivalent structures. The Burgers vectors of such dislocations can have considerably smaller magnitudes than $\boldsymbol{d}^{\mathrm{sc}}$ dislocations, and examples of the dissociation of perfect $\boldsymbol{d}^{\mathrm{sc}}$ dislocations into partial dislocations have been observed experimentally (Pond 1977).

The new step in the procedure to predict a dislocation network is to consider the decomposition of $\boldsymbol{d}^{\mathrm{sc}}$ vectors in the b-net. Figure 8 (*b*) shows an example, in the hexagonal boundary considered above, where the black crystal has been displaced by $\boldsymbol{p}'_{\mathrm{i}}$ from the rank 1 reference position. The rank 1 bicrystal could have point symmetry 62′, and the displaced structure has point symmetry 1 only and rank 12. The resulting dislocation network contains 12-, 6- and 4-fold nodes. Naturally the contrast of the dislocation lines in electron micrographs would vary, depending on the diffraction condition and the size and orientation of the Burgers vectors.

Relative displacements $\boldsymbol{p}'_{\mathrm{i}}$ corresponding to structures with rank lower than 12 cause certain dislocations to 'fade out' from the network. Figures 4 (*c*) and (*d*) correspond to two different

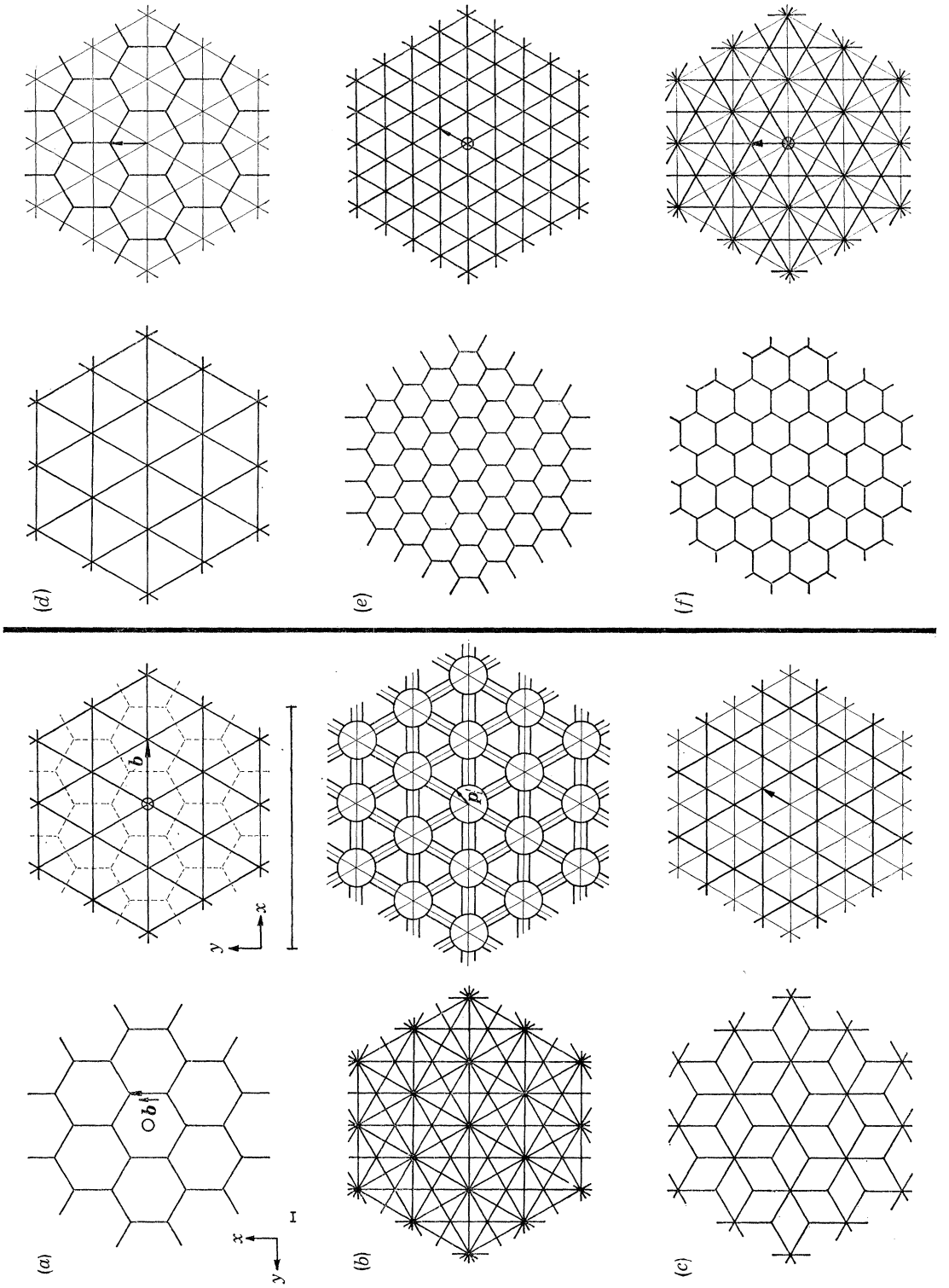

FIGURE 8. Secondary dislocation networks and their corresponding b-nets in a twist bicrystal with a small angular deviation from a coincidence orientation. The sequence (*a*)–(*d*) illustrates the variation of network appearance depending on the rank of the interface structure: (*a*) rank 1, (*b*) rank 12, (*c*) and (*d*) rank 3. The networks shown in (*e*) and (*f*) show the networks expected if two interface structures are stable; (*e*) combination of interface structures in (*a*) and (*c*) are stable, (*f*) structures as in (*a*) and (*d*) are stable.

rank 3 structures. Thus, the form of the dislocation network depends on the rank o fthe underlying structure. However, the symmetry of the network, including the relative magnitudes of Burgers vectors, is unaltered by this. The symmetry of dislocation networks can be classified according to the seventeen space groups of two-dimensional networks (Shubnikov & Koptsik 1974). In the present case the symmetry of the b-nets and dislocation networks is always $p6mm$. It is interesting to note that b-nets are always planar isogons, i.e. all vertices are identical or mirror related, and networks are figures complementary to these called plane isohedra, i.e. figures comprising equal polygons fitting the plane with no gaps (Shubnikov & Koptsik 1974).

Further changes to network tessellation occur if more than one non-equivalent interface structures are stable. Figures 8 (e) and (f) show examples of network tessellations when the reference structure (rank 1) and the rank 3 structures in figures 8 (c) and (d) respectively are stable and have similar γ. We note that the symmetry of the network remains $p6mm$.

6. Discussion

The foregoing sections have shown how the space and/or point symmetry of bicrystals can be classified. In general, bicrystals consisting of two different phases tend to be low symmetry structures but grain boundary structures can exhibit high symmetry. It is felt that the use of colour symmetry has helped to simplify various aspects of bicrystal symmetry, especially in the discussion of equivalent structures. It has also been shown why an understanding of the symmetry of dichromatic patterns is valuable; these symmetry elements govern the symmetry of all possible bicrystals that can be created from a given dichromatic pattern, and the Burgers vectors of interfacial dislocations correspond to anti-translations in dichromatic patterns rather than interfacial translation symmetry in bicrystal structures.

Several results of interest may be noted from this investigation of bicrystal symmetry. For example, it is clear that classical coincidence grain boundary structures are not necessarily unique in the sense that other structures with equally high symmetry obtained by relative displacement from the coincidence structure can exist on a given interface. Also, interface structures based on c.s.l. can have identical point symmetry even though, for example, $[hkl]$ is $\langle 001\rangle$ in one case and $\langle 011\rangle$ in the other. As an illustration, consider a twist boundary with $[hkl] = [001]$, such as is shown in figure 3 (b) where $\boldsymbol{p}_1' = \frac{1}{2}\boldsymbol{b}_2$; this bicrystal has the layer space group $p2_1'2'2$, while a bicrystal with $[hkl] = [011]$, such as is shown in figure 1 (d) has the space group $p2_1'2_1'2$. Thus, by invoking Neumann's principle, we see that the symmetry of certain physical properties of these (001) and (011) twist boundaries could be identical. It has also been shown that an experimental investigation of the tessellated form of secondary dislocation networks accommodating small angular deviations from coincidence misorientations could give information concerning the presence of equivalent interfacial structures.

A useful application of bicrystal symmetry is for the investigation of interfacial structure by atomistic calculation using computers. The nature of atomistic relaxations will depend on the symmetry of the bicrystal. Consider a bicrystal modelled in a computer with central forces as an approximation to interatomic forces. The symmetry of the force field, i.e. the interaction of all forces in the bicrystal, must be at least as high as the bicrystal symmetry. In other words, if an initial bicrystal is constructed with a given relative displacement no forces can act to destroy any of the symmetry elements present in the initial structure. Therefore, for example, any forces acting which tend to give rise to further relative displacement of the two crystals, must act to

conserve the initial symmetry and hence must act parallel to the directions of relative displacement which conserve those symmetry elements as explained in §§ 3 and 4. If an initial bicrystal contains two non-collinear axes 2′, for example, no further relative displacement can occur, because any movement would destroy some of this symmetry. Thus, we can deduce, for example, that (001) twist boundary structures with relative displacements $\boldsymbol{p}_i' = 0$, $\frac{1}{2}\boldsymbol{b}_1$ and $\frac{1}{2}(\boldsymbol{b}_1 + \boldsymbol{b}_2)$ (i.e. points O, A and B in figure 7) are metastable structures. Avoiding such metastable structures, or checking their stability to further small relative displacements, is a well known problem in atomistic calculations. It is suggested that consideration of bicrystal symmetry can streamline the design of algorithms to avoid calculated structures caught in the ‘symmetry trap’.

It is possible that certain symmetry elements are associated with bicrystal stability in a way analogous to the well known role of points with inversion symmetry in simple lattices. For example, consider the symmetry of the $\Sigma = 5$ (310) and (210), and $\Sigma = 9$ (221) bicrystals computed to be stable according to figure 5. It is particularly noteworthy that for all of these tilt structures the ordinary mirror plane perpendicular to the tilt axis has been conserved. The bicrystals represented in figure 5 are composed of f.c.c. crystals. However, simulations of tilt bicrystals comprised of b.c.c. (Bristowe & Crocker 1975) and orthorhombic polyethylene (Geary & Bacon 1976) show identical behaviour; in both of these cases the holosymmetric bicrystals have layer space group $p2'mm'$ but relax to stable configurations with the layer space group $p1m1$, by relative displacements perpendicular to the tilt axis. In general, no restoring forces arise as a result of relative displacements $\boldsymbol{p}_i'$ which are perpendicular to the tilt axis. Exceptions to this rule are the holosymmetric structures such as $\Sigma = 5$ (310) β, $\Sigma = 5$ (210) δ, $\Sigma = 9$, (221) α, β, (see figure 5).

Since ordinary mirror symmetry appears to be associated with stability of bicrystals in a direction perpendicular to the mirror plane, it is expected that bicrystals with more than one non-parallel ordinary mirror plane are stable with respect to any additional relative displacement. An example where this is true is the coherent (111) twin boundary ($\Sigma = 3$) between f.c.c. crystals at the classical coincidence relative displacement; the layer space group in this case is $p\bar{6}'m2'$ (this space group could alternatively be written $p3/m'm2'$ which has the advantage that it is consistent with the premise set down in § 4.1 that only non-colour reversing rotation axes can be normal to an interface plane. Note also that the interface plane contains neutral bases in this case).

The coherent (111) $\Sigma = 3$ bicrystal is the most highly symmetric possible, and we note that its point symmetry does not include inversion symmetry. No bicrystal can include points of inversion symmetry in its unique plane since the existence of these would require that the basic translation vectors and their orientation be identical on either side of that plane. This feature of bicrystals may be contrasted with the important role of inversion symmetry in the stability of structures based on simple lattices. Certain faulted single crystals may be regarded as ‘bicrystals’ and there can be points of inversion in the fault plane. Two examples are antiphase domain boundaries and f.c.c. crystals separated by a stacking fault on (111); in the latter case the layer space group is $p\bar{3}'m1$.

The role of symmetry elements in the stability of bicrystals may also be discussed in terms of γ surfaces. The γ surface for a bicrystal is a contoured surface based on the in-plane W–S cell such that the height of the surface at a point corresponding to a structure with fixed $\boldsymbol{p}_i'$ is proportional to γ for that structure (local atomic relaxation is allowed for each structure). If a holosymmetric bicrystal has both translation symmetry and point symmetry higher than 1, equivalent bicrystal structures can exist. Thus, equivalent points in the W.–S. cell will lead to points of equal height on the γ surface. The gradient of the surface $\mathrm{d}\gamma/\mathrm{d}(\boldsymbol{p}_i')$ at any point corresponds to the overall force

tending to cause additional relative displacement from the structure corresponding to $\boldsymbol{p}_i$. Evidently $d\gamma/d(\boldsymbol{p}'_i(\text{perp})) = 0$ for all stable structures described in figure 5, where $\boldsymbol{p}'_i(\text{perp})$ is a relative displacement in a direction perpendicular to the ordinary mirror planes. At points on the γ surface corresponding to structures with more than one non-parallel symmetry axis parallel to the interface $d\gamma/d(\boldsymbol{p}'_i) = 0$, i.e. the position must be a local minimum or maximum on the γ surface. Local maxima correspond to metastable structures caught in the symmetry trap whereas local minima correspond to structures with some measure of stability. Thus, symmetry positions on a γ surface must correspond to stationary points, but this does not preclude the possibility of deep local minima, i.e. favourable structures, occurring at points corresponding to bicrystals with no point symmetry.

The authors are grateful to Professor Sir Charles Frank, F.R.S., and Professor J. W. Christian, F.R.S., for helpful comments, to Professor D. Hull for encouragement, and one author (W.B.) wishes to thank the Science Research Council for financial support.

References

Balluffi, R. W. 1972 *Surf. Sci.* **31**, 68.
Bollmann, W. 1970 *Crystal defects and crystalline interfaces*. Berlin: Springer–Verlag.
Bristowe, P. D. & Crocker, A. G. 1975 *Phil. Mag.* **31**, 503.
Bristowe, P. D. & Crocker, A. G. 1978 *Phil. Mag.* A **38**, 487.
Darby, T. P. ,Schindler, R. & Balluffi, R. W. 1978 *Phil. Mag.* A **37**, 245.
Geary, N. A. & Bacon, D. J. 1976 *Nucl. Metall.* **20**, 479.
Grimmer, H., Bollmann, W. & Warrington, D. H. 1974 *Acta crystallogr.* A **30**, 197.
International tables for X-ray crystallography 1969 Birmingham: Kynoch Press.
Loeb, A. L. 1971 *Colour and symmetry* New York: John Wiley
Neronova, N. N. & Belov, N. V. 1961 Soviet Physics – Crystallography **6**, 1.
Nye, J. F. 1969 *The physical properties of crystals*. Oxford University Press.
Pond, R. C. 1977 *Proc. R. Soc. Lond.* A **357**, 471.
Pond, R. C. 1979 *Phil. Mag.* A **39**, 679.
Pond, R. C. & Vitek, V. 1977 *Proc. R. Soc. Lond.* A **357**, 453.
Pond, R. C., Smith, D. A. & Vitek, V. 1979 *Acta metall.* **27**, 235.
Smith, D. A., Vitek, V. & Pond, R. C. 1977 *Acta metall.* **25**, 475.
Shubnikov, A. V. & Koptsik, V. A. 1974 *Symmetry in science and art*. New York: Plenum Press.
Warrington, D. H. & Bollmann, W. 1972 *Phil. Mag.* **25**, 1195.
Warrington, D. H. & Bufalini, P. 1971 *Scripta metall.* **5**, 771.

PHILOSOPHICAL TRANSACTIONS OF THE ROYAL SOCIETY A MATHEMATICAL, PHYSICAL & ENGINEERING SCIENCES